International Journal of Clinical Chemistry and Laboratory Medicine (IJCCLM)
Volume 5, Issue 3, 2019, PP 6-18
ISSN No. (Online) 2455-7153
DOI: http://dx.doi.org/10.20431/2455-7153.0503002
www.arcjournals.org

The Morphology and Proteomics Variance Analysis of QSG-7701 and QGY-7703 Cell Lines after Cisplatin Treatment

Peidi Yin[2], Jianliang Chen[3], Guangxu Cao[2], Yusheng Fang[3], Bin Du[2], Mao Fang[1*]

[1]*Department of Pathology, School of Basic medical sciences, Guangzhou Medical University, Guangzhou, China*

[2]*Department of Pathology, Medical school of Jinan University, Guangzhou, China*

[3]*Department of Pharmaceutical Engineering, South China Agricultural University, Guangzhou, China*

Corresponding Author:** ***Mao Fang, *Department of Pathology, School of Basic medical sciences, Guangzhou Medical University, Guangzhou, China*

Abstract: *Hepatocellular carcinoma (HCC) is one of the most common human malignancy cancers and lacks the specific diagnosis targets and good treatment method. Herein, two abnormal expressed proteins in tumour cells were reported which can affect cell proliferation by proteomics technology combined with bioinformatics analysis methods. The QSG-7701 hepatocyte cell line and QGY-7703 hepatocyte cancer cell line which have the same genetic background were used as experiment samples, the mechanisms of tumour development and apoptosis induced by cisplatin (CDDP) were researched at the level of isolated culture cells. The QGY-7703 apoptosis model by CDDP were established and compared with QSG-7701 and QGY-7703 in morphology and growth characteristics. Then the proteins were extracted from these samples and the differentially expressed proteins were inspected thought 2-DE software analysis. Finally, two target proteins which were specially expressed in QGY-7703 and lacked in QSG-7701 and QGY-7703 after treatment with CDDP, were certified and analysed by mass spectrometry technology and bioinformatics method.*

Keywords: *Primary liver cancer; Proteomics; Cisplatin; Apoptosis*

1. INTRODUCTION

Primary hepatocellular carcinoma (HCC) refers to cancer that occurs in hepatocytes and intrahepatic bile duct epithelial cells, which has a high incidence in Asia and Africa very popular in Asia and Africa. Compared with other tumours, the occurrence and development of HCC is a complex process involving multiple genes in the body and multi-step synergy. It has the characteristics of insidious onset, long incubation period, high degree of malignancy, rapid progress, easy transfer, and poor prognosis [1]. Recently, the molecular mechanism of HCC pathogenesis remains unclear, lacking reliable molecular markers for early diagnosis and treatment. Radiotherapy, chemotherapy, and surgery have long been common methods of curing tumours. Due to the tolerance to multiple chemotherapeutic drugs, difficulties of early diagnosis, and poor prognosis of advanced patients, the choice of treatment options for liver cancer is greatly limited [2]. Surgical resection has been widely recognized as the best means of radical liver cancer, however, the overall 5-year survival rate after liver cancer surgery is not high. The annual survival rate is not high. Epidemiological data showed that the 5-year survival rate of large liver cancer is only 34.6%, while small liver cancer is only 62.9% [3]. Although a series of HCC

molecular markers such as alpha-fetoprotein (AFP) and carcinoembryonic antigen (CEA) were used clinically, the detection sensitivity and specificity are not ideal [4, 5]. Therefore, exploring the molecular mechanism of liver cancer development and finding the target molecules have important theoretical guidance and clinical application significance for the diagnosis and treatment of this malignant tumour.

The cisplatin (CDDP) is the first platinum anti-tumour drug in the market, it was used clinically in 1969. Due to its broad anti-cancer spectrum and strong anti-tumour activity, the CDDP is a very promising anti-cancer drug, which is widely used in various solid tumours. The CDDP binds to biomacromolecules in cells in the form of hydrated cations to form DNA cross-linking, intra-chain cross-linking, DNA-protein cross-linking, can disrupt DNA replication and inhibit cell division [6]. The CDDP can also accumulate in mitochondria to increase the ability of mitochondria to produce reactive oxygen species (ROS), causing cell death [7, 8]. In addition, the CDDP raises ROS and activates JNK and p38MAPK oxidative stress kinase pathways leading to apoptosis [9]. While in some cells, it stimulates ROS and activates the ERK signaling pathway to induce apoptosis [10]. The ERK1/2 signaling pathway (Ras/Raf/MEK/ERK) is a classical MAPK signal transduction pathway [11], That is, when the growth factor binds to a specific receptor on the cell membrane, it causes a series of protein knots. In combination with enzymatic phosphorylation, ERK1/2 is specifically activated, and activated ERK1/2 regulates cell proliferation by phosphorylating nuclear transcription factors. The ERK1/2 pathway also antagonizes the pro-apoptotic activity of the JNK and p38 pathways and promotes cell survival. Blocking the activation of the ERK1/2 signaling pathway can significantly inhibit cell proliferation and promotes apoptosis [12], which suggested that the specific inhibitor of this pathway has important application value for cancer treatment.

Proteomics refers to all the corresponding proteins expressed by the genome of a cell or a tissue [13]. Compared with liver tumor tissues, liver tumor cell lines are more readily available and have a single component and high comparability which are widely used in proteomics analysis in research. A large of results reported indicated that the regulatory pathways of chaperone proteins and tumor-associated proteins involved in carcinogenesis, growth and metastasis can be identified by analyzing the function of liver cancer cell lines [14. 15], thus demonstrating that proteomics of hepatoma cell lines is feasible in tumor research.

We selected the hepatocyte cell line QSG-7701 and the hepatoma cell line QGY-7703 as research samples for systematic morphological and proteomic studies of HCC in vivo. The hepatocyte cell line QSG-7701 is derived from the adjacent normal tissues of the tumour, and the latter from cancerous tissues belonging to liver cancer cells. Wang et, al. established the cell lines and published [16, 17], and the two cell building processes and phenotypic characteristics were described in detail in the literature. Because QSG-7701 hepatocytes and QGY-7703 liver cancer cells are from the same donor, the genetic background is the same, eliminating the complex biological background caused by individual differences in organisms, and it is easy to find proteins directly related to diseases through proteomics techniques. QGY-7703 was processed to observe the changes in the morphology, nuclear DNA and proteomic levels of QGY-7703 cells after drug treatment, which provided a basis for elucidating the mechanism of CDDP-induced cell death and screening new therapeutic molecular targets. Previously, the genomes of DNA and mRNA levels of two cell lines were also studied [18-21], but the use of traditional two-dimensional gel electrophoresis technology to study the proteome level of two cells has not been reported.

2. Materials and Methods

2.1. Cell Culture

QSG-7701 hepatocyte cells and QGY-7703 liver cancer cells were provided by Shanghai Institute of Cell Culture Collection, Chinese Academy of Sciences and were cultured in RPMI-l640 medium (1640) supplemented with 10% foetal bovine serum (FBS) and 1% penicillin/streptomycin. All reagents and solvents were purchased from Gibco (Carlsbad, CA).

2.2. Reagents

IPG dry strip (13 cm, pH 3-10), mineral oil, IPG buffer (pH 3-10), Acrylamide, Dithiothreitol (DTT) were purchased from Amersham bioscience (USA). Ammonium persulfate, sodium dodecyl sulfate (SDS), N, N, N'N'-tetramethylvinylamine (TEMED), dimethyl sulfoxide (DMSO), Hoechst No. 33324 fluorescent dye, ribonucleic acid Enzyme A, ethidium bromide (EB), ethylenediaminetetraacetic acid (EDTA), chromatographic grade trifluoroacetic acid (TFA), acetic acid, mass spectrometry grade α-cyano-4-hydroxyphenylacrylic acid (CHCA), ammonium hydrogencarbonate , potassium ferricyanide (K3Fe(CN)6) were were purchased from Sigma (USA). Urea, thiourea, glycerin, low melting point agarose, Tris, glycine, Coomassie Brilliant Blue R-250, Coomassie Brilliant Blue G-250, Benzylsulfonyl fluoride (PMSF), 3-(3-cholamidopropyl-diethylamine)-propanesulfonic acid (CHAPS) were purchased from Amresco (USA). Hematoxylin, eosin and agarose gel were purchased from Sangon Biotech (China). Bovine serum albumin and bromophenol blue were purchased from Guangzhou Weijia (China). Fetal bovine serum, penicillin and streptomycin were purchased from Institute of Microbiology, Chinese Academy of Sciences (China). DL, 2000TM DNA Marker, 6X loading Buffer were purchased from TAKARA (Japan). CDDP (20mg) was purchased from Dezhou Dehua pharmaceutical co., LTD (China). Mass spectrometry trypsin was purchased from Promega (USA). Chromatographic grade acetonitrile (ACN) was purchased from Fisher (USA). ZipTip®C18 was purchased from Millipore (USA).

2.3. Growth Curve Determination

QSG-7701 and QGY-7703 cells were taken and resuspended by centrifugation to prepare a cell suspension. Prepare a cell suspension of 3×104 cells/mL after counting by the blood cell counting plate, inoculate 3 mL of each bottle in a 20 mL cell culture flask, and change the medium every other day for 7 days. Take 3 bottles for counting every day and take the average as a result. The growth time was plotted on the horizontal axis and the number of cells was plotted on the vertical axis (logarithm), and the doubling time was calculated according to the following formula.

$$Td=\Delta t\times lg2/(lgNt-lgN0)$$

Define Td as the doubling time, Δt as the number of counting intervals, Nt as the theoretical observation at any point in the logarithmic growth phase, and N0 as the theoretical initial value of the logarithmic growth phase.

2.4. Cell Morphology Observation for QGY-7703 Cells Treated by CDDP

The logarithmic growth phase QGY-7703 cells were prepared into 3×10^5 cells/mL single cell suspension, inoculated into 12-well plates, and 2 mL medium was added to each well then cultured at 37 ° C , 5% CO_2 . When the cells are covered with 70% of the bottom, discard the medium and add 2 mL new medium containing different concentrations of CDDP (0 μg/ml, 2 μg/ml, 4 μg/ml, 8 μg/ml) for each. Three replicate wells were set for each concentration. After 24 h, the cell slides were removed and HE staining and Hoechst 33324 staining were performed and observed under the microscope.

2.5. Agarose Electrophoresis for Detection DNA Ladder

QGY-7703 cells cultured in different concentrations of CDDP (0 μg/ml, 2 μg/ml, 4 μg/ml, 8 μg/ml) for 24h were harvested, and the DNA was extracted following a protocol [22]. Observe and photograph the agarose gel by a gel imaging system after electrophoresis.

2.6. The Protein Two-Dimensional Electrophoresis and Mass Spectrometry

The protein of cells was extracted following a protocol [23]. And the Two-dimensional electrophoresis following a protocol [24]. The two-dimensional gel electrophoresis silver-stained gel was placed on an ARCUS image scanner for gel scanning to obtain a clear 2-D image. The image was analyzed by the PDQuest8.01 gel image analysis system for spot detection, background subtraction, matching, quantification, and spot position coordinates. The volume of protein spots on the gel was expressed as the relative density value of each point. After the above treatment, the protein spots in the gel spectrum of a certain sample were significantly enhanced compared with the gels of other samples (the expression level of the corrected points was more than 2 times), and the gel profiles of the same group of 3 gels showed the same change, then we can regard it as a differential protein point. Statistical analysis of all data was performed on SPSS 16.0 software. The control group QSG-7701 cells and the untreated QGY-7703 cells, the untreated QGY-7703 cells and the CDDP treated QGY-7703 cells were matched and analyzed to obtain differentially expressed protein spots, and some protein differences were observed in two-dimensional electrophoresis and we marked them on the map.

The samples were treated and spotted onto a clean, dry MALDI sample target following a protocol [25]. Place the sample target in a clean space, dry at room temperature, blow the sample surface with compressed nitrogen, and then input the sample target into an ABI 4800 MALDI-TOF/TOF mass spectrometer. The operating parameters of the nitrogen laser (337 nm, pulse width 3 ns) are as follows: reflection, positive charge mode, acceleration voltage 25 KV. The extraction voltage is 64.5% and the ion delay is extracted for 150 ns. Internal standard calibration, laser intensity 6000, bombardment of 1200 times per sample, random selection of 40 points, bombardment of each point 30 times, obtaining peptide mass fingerprinting (PMF). Database retrieval of mass spectrometry PMF using Mascot software, and the highly reliable results with a protein score greater than 95% was obtained by searching the MSBInr and Swissprot databases using the MS/MS combined model (The species database is a human database with a molecular weight range of 800-4000 and the mass tolerance error is 50 ppm and there must be more than 4 peptide matches).

2.7. Bioinformatics Analysis

The first-order amino acid sequence of the protein was obtained by searching the Swiss-Prot database based on the mass spectrometric identification of the protein sequence number. The SAWISS-MODEL online tool was used to predict the three-dimensional structure of the protein. The hydrophobicity/hydrophilicity of the protein amino acid sequence was analyzed using Protscale software (http://web.expasy.org/protscale/). The secondary structure predicted by Chou-Fasman and Gamier-

Robson methods which are modules in Protean of DNAstar software; the protein flexibility was analyzed by the Karplus-Schulz method; the protein surface accessibility was analyzed by the Emini method; and the protein antigenicity index was analyzed by the Jameson-Wolf method. The ability of proteins to bind

to MHC class II molecules and specific ligands were predicted by ProPred software (http://www.intech.res.in/raghava/propred/index.html) in conjunction with NetMHCII Server 2.2 (http://www.cbs.dtu.dk/services/NetMHCII/).

3. RESULTS

3.1. Comparative Analysis of QSG-7701 and QGY-7703

To compare the proliferation performance of the QSG-7701 cell line and the QGY-7703 cell line, the growth curves of the two were determined (Fig. 1A). The doubling time of QSG-7701 cells and QGY-7703 cells was at 21.6 h and 19.6 h respectively. The maximum proliferation multiples of the two cell lines were 12.6 and 14.1 respectively. The result showed that the proliferation of QGY-7703 cells is slightly stronger than that of QSG-7701 cells, and the logarithmic growth phase is almost the same, indicating that QSG-7701 cells have similar cancer cell characteristics in proliferation performance. The cell slides of QSG-7701 and QGY-7703 were taken out and subjected to conventional HE staining to observe the morphological differences between the two cell lines (Fig. 1B). The result showed that both QGY-7703 and QSG-7701 have multiple nucleoli, which have different binding properties to dyes. QSG-7701 cells are mostly round, with multiple nucleoli, and the cytoplasm is slightly purple, indicating easily binding to acid dyes (picture a). While the QGY-7703 cells have many fusiform shapes and large nuclear-to-cytoplasmic ratio (picture b), a lot of large cells are fused by multiple cells, and the number of nucleoli is more and clearer. The cytoplasm is evenly purpled, indicating that it is easily binging to basic dyes.

3.2. Inducing Apoptosis of QGY-7703 Cells by CDDP Treated

QGY-7703 cells were treated with different concentrations of CDDP for 6 and 24 h, and the number of adherent cells after CDDP treated was evaluated by cell counting. As shown in Fig. 2A, after CDDP treatment for 6 h and 24h, the number of adherent cells no longer decreased when the concentration reached 8 μg/ml or more. The decrease in the number of cells treated with CDDP for 24 h was more pronounced, the result showed that the CDDP inhibited the proliferation of QGY-7703 in a concentration-dependent manner. The morphological changes of QGY-7703 cells after CDDP treatment for 24 h were

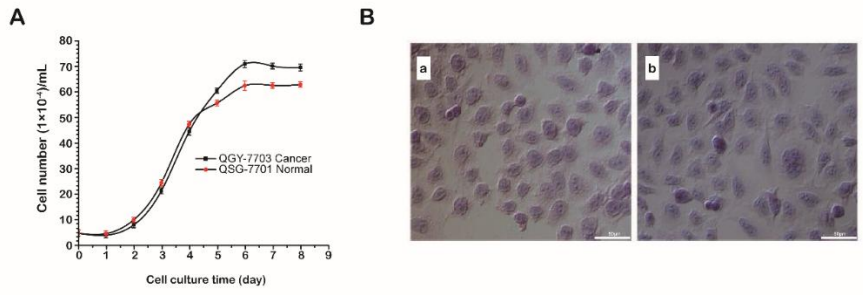

Fig1. *(A) Growth curves of QSG-7701 and QGY-7703. QSG-7701 cells have similar cancer cell characteristics in proliferation performance. (B) Cell morphology of QSG-7701 and QGY-7703 cells. The images are magnified 400× (the scale bars within the photomicrographs are 50 microns in length).*

observed by HE staining (Fig. 2B). The result showed that the control group of QGY-7703 cells grew well, mostly fusiform and triangular, and the cells were arranged in a single layer with clear boundaries. The cells were plumpness and round in size and vigor under the inverted microscope before staining.

After treated with 2, 4, 8 μg/mL CDDP for 24 h, the number of adherent cells decreased significantly with the increase of concentration, and the cells were obviously shrunk, and the transparency was decreased under the inverted microscope before staining, showing some features in the early stage of apoptosis. We used Hoechst 33324 to stain QGY-7703 cells treated with different concentrations of CDDP for 24 h. The stained cells showed typical apoptotic features such as chromatin condensation and

chromatin edge collection under fluorescence microscope. As shown in Fig. 2C, the untreated QGY-7703 cells showed uniform blue fluorescence (picture a). The 2 μg/mL, 4 μg/mL CDDP treatment group blue fluorescence brightening, chromatin condensation and edge aggregation apoptotic features (picture b and c). The results of the 8 μg/ml CDDP treatment group showed a significant decrease in cells, and some of the nuclei were fragmented into fragments, indicating late apoptosis characteristics (picture d). DNA fragmentation is a typical feature of apoptosis. We used electrophoresis to analyze nuclear DNA of QGY-7703 cells after CDDP treatment (Fig. 2D). The result showed that after 2 μg/mL and 4 μg/mL CDDP treatment for 24 h, a weak DNA ladder appeared, and after 8 μg/mL CDDP for 24 h, a clear DNA ladder appeared. In the contol group, there is only one complete DNA band. We indicated that the CDDP can induce apoptosis in QGY-7703 cells.

3.3. Differentially Expressed Protein Analysis

As shown in Fig. 3A, different lysates were used to extract proteins from QSG-7701 group, untreated QGY-7703 group and CDDP treatment QGY-7703 group. The 2-DE silver staining patterns of the three protein samples were established under the same conditions. Analysis of the 2-DE map established by Lysis Buffer 1 using PDQuest8.01 software showed that QSG-7701 (picture a) had 790 protein spots on the 2-DE gel. There are 815 protein spots on the 2-DE gel of untreated QGY-7703 (picture d). After CDDP treatment, QGY-7703 (picture g) has 636 protein spots on the 2-DE gel.

PDQuest8.01 software was used to analyze the two-dimensional electrophoresis patterns of QSG-7701 and QGY-7703 cell proteins which were extracted with lysate 1. The difference in expression levels was more than 2 times as the difference point. The results showed that 48 differentially expressed protein spots were observed, of which 24 proteins were expressed only in QGY-7703 cells, and 9 proteins were

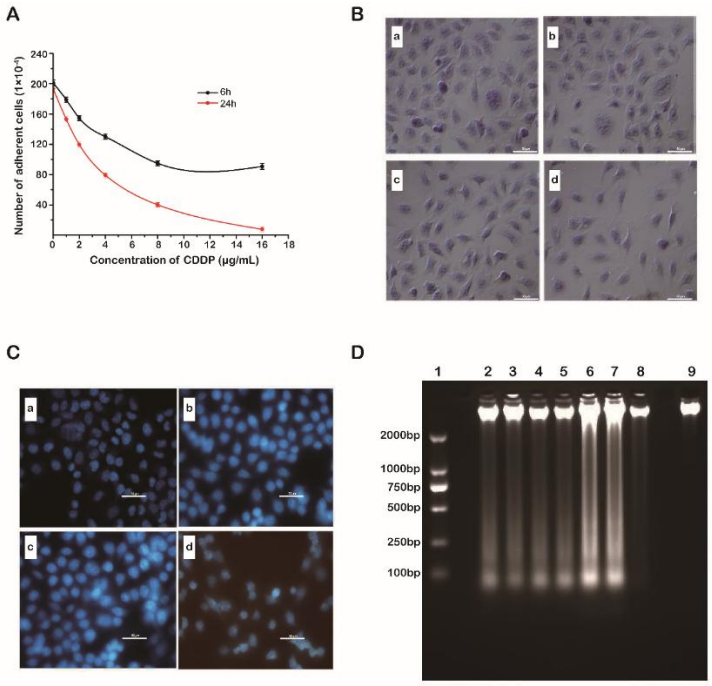

Fig2. *(A) Cell number of adherent cells after CDDP treated. (B) Cell morphology of QGY-7703 cells after CDDP treated for 24h. The a is for control group; b is for 2 μg/mL CDDP treatment group; c is for 4 μg/mL CDDP treatment group; d is for 8 μg/mL CDDP treatment group. The images are magnified 400× (the scale bars within the photomicrographs are 50 microns in length). (C) Hoechst 33324 staining to observe cell morphology. The a*

is for control group; b is for 2 μg/mL CDDP treatment group; c is for 4 μg/mL CDDP treatment group; d is for 8 μg/mL CDDP treatment group. The images are magnified 400× (the scale bars within the photomicrographs are 50 microns in length). (D) The DNA Ladder analysis of QGY-7703 cells. The lane 1 is for DNA marker; the lane 2 and 3 are for 2 μg/mL CDDP treatment group ;the lane 4 and 5 are for 4 μg/mL CDDP treatment group; the lane 6 and 7 are for 8 μg/mL CDDP treatment group; the lane 8 and 9 are for control group.

only expressed in QSG-7701 cells. There were 15 proteins expressed in both cells, 4 of which up-regulated in QGY-7703 cells and 11 down-regulated. Analyze the proteins of untreated QGY-7703 cells and CDDP treated QGY-7703 cells in the same way. The results showed that 48 differentially expressed protein spots were observed, of which 18 proteins were expressed only in untreated QGY-7703 cells, and 9 proteins were only expressed in CDDP treated QGY-7703 cells. There were 21 proteins expressed in both cells, 7 of which up-regulated in QGY-7703 cells and 14 down-regulated. The two-dimensional electrophoresis patterns with lysate 1, 2, and 3 were comparative analyzed (Fig. 3B). The result revealed two protein spots missing expressed in QGY-7703 cells and 4 μg/mL CDDP treated QSG-7701 cells, which expressed in untreated QGY-7703 cells (as shown with the black arrows).

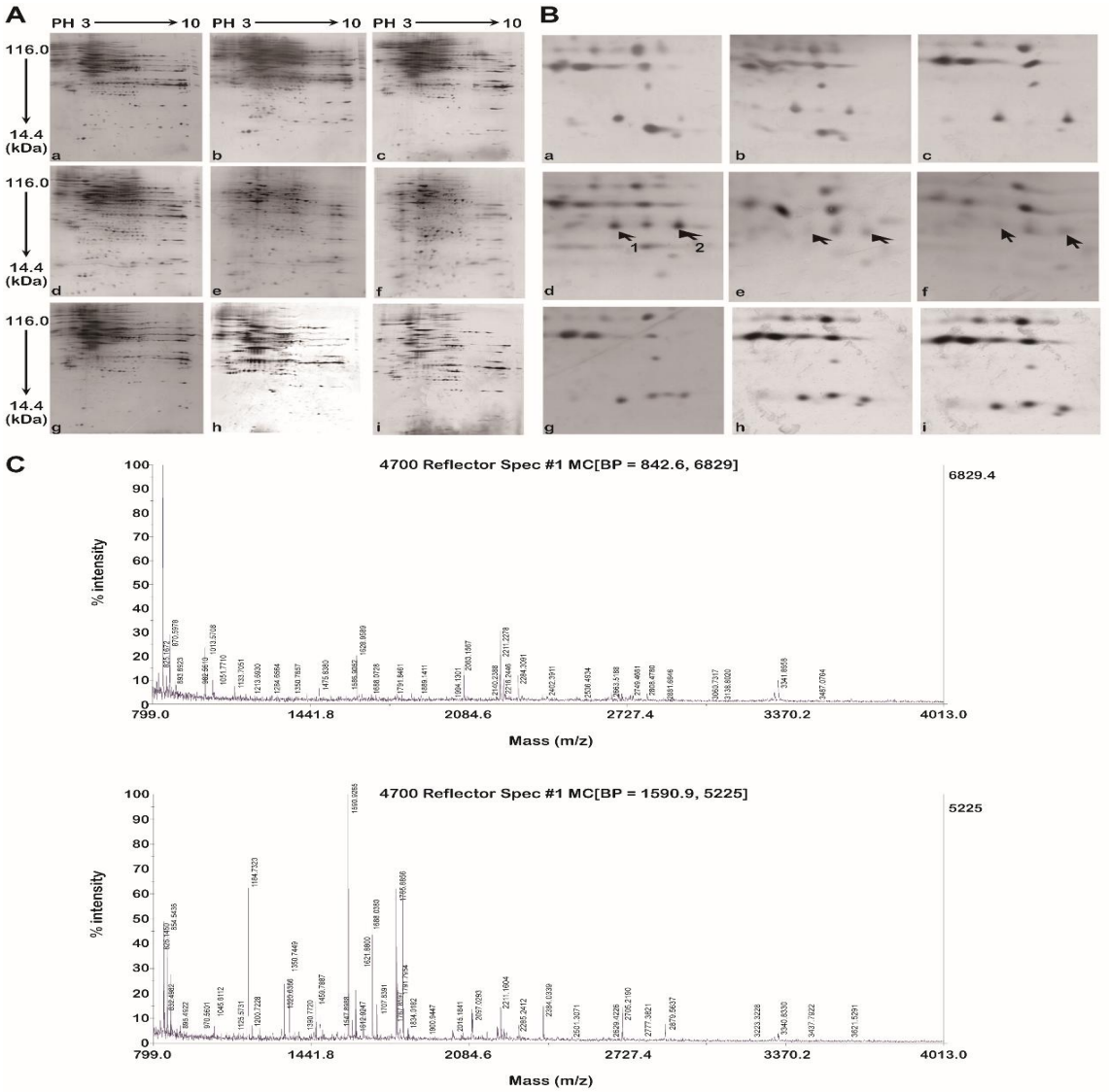

Fig3. *(A-B) 2-DE map of cellular proteins from each group and local differentially expressed protein spot enlargement. The left column (a, d, g) showed the results with lysate 1; the middle column (b, e, h) showed the results with lysate 2; the right column (b, e, h) showed the results with lysate 2. The first row showed the results*

of QSG-7701 group; the second row showed the results of untreated QGY-7703 group; the third row showed the results of 4 μg/mL CDDP treated QGY-7703 group. The black arrows showed the two QGY-7703 cell-specific protein spots. (C) The PMF of specific protein spots. The picture above is for the No.1 protein spot , while the picture below is for the No.2 protein spot.

The two QGY-7703 cell-specific proteins were digested into peptides with protease. The peptide mass fingerprinting (PMF) was obtained by MALDI-TOF/TOF mass spectrometry, as shown in Fig. 3C. The MASCOT software was used to search in the NCBInr and SWISS-PROT databases after combining the primary and secondary mass spectra obtained by mass spectrometry.

3.4. Bioinformatics Analysis

The amino acid sequence of Acyl-protein thioesterase 2 (APT-2) and 17-beta-hydroxysteroid dehydrogenase 10 (17-beta-HSD 10) were found by searching the protein sequence number O95372 and Q99714 in the Swiss-Prot database. The hydrophobicity/hydrophilicity of the APT-2 and 17-beta-HSD 10 amino acid sequences were analyzed by Protscale software (Fig. 4A).

The results showed that, in APT-2, the lowest score of the polypeptide chain was -1.600 and the highest score was 2.356, most of which were positive; in 17-beta-HSD 10, the lowest score of the polypeptide chain was -2.711 and the highest score was 2.089, most of which were positive. According to the lower the amino acid score, the stronger the hydrophilicity and the higher the score, the stronger the hydrophobicity. It illustrated that APT-2 and 17-beta-HSD 10 are highly hydrophobic and should be hydrophobic proteins. As shown in Fig. 4B(a), APT-2 contains 9 alpha helices, 10 beta sheets and 10 random coil structures, and there are 14 corner structures between the alpha helices and the beta sheets;

are 13 corner structures between the alpha helices and the beta sheets. As shown in Fig. 4B(b), the APT-2 protein has 16 flexible regions with concentrated N-terminal, C-terminal and intermediate sites, while the 17-beta-HSD 10 protein has 13 flexible regions and the distribution is relatively uniform. According to the antigenicity index of the protein, it is known that the two proteins have multiple potential epitopes,as shown in Fig. 4B(c). It can be seen from Fig. 4B(d) that the surface accessibility of multiple residues of the two proteins are relatively large. B cell epitopes generally have a high antigenic index, a large surface accessibility, and are mostly characterized by a flexible corner structure. Combining the results of 4 methods, it is speculated that the amino acid residue (82-89, SPDAPEDE) segment is the APT-2 dominant B cell epitope, and the amino acid residue (137-145, NVIRLVAGE) segment is the 17-beta-HSD 10 dominant B cell epitope which can be used as the focus of subsequent analysis.

As shown in Fig. 4C, there are three nonapeptides which have strong binding ability to MHC class

II molecules in APT-2 (affinity(nM) <50), and 24 nonapeptides which have weak binding ability to MHC class II molecules (50<affinity(nM)<500). It was also found that the strong binding ability nonapeptide (affinity (nM) <50) is associated with the HLA-DRB1_0101 and HLA-DRB1_0701 genotypes; while there are three nonapeptides which have strong binding ability to MHC class II molecules in 17-beta-HSD 10 (affinity(nM) <50), and 37 nonapeptides which have weak binding ability to MHC class II molecules (50<affinity(nM)<500). It was also found that the strong binding ability nonapeptide (affinity (nM) <50) is associated with the HLA-DRB1_0701 and HLA-DRB5_0101 genotypes.

ProPred was used to predict specific ligands for binding to MHC class II molecules in APT-2 and 17-beta-HSD 10, the results in Fig. 4D showed that APT-2 contains multiple specific peptides that bind to MHC class II molecules and 72 specific P1 site anchoring bases. As the results showed, the strongest

recognition sites in APT-2 which related with HLA-DRB1_0101 and HLA-DRB1_0701 are amino acids 182 and 142 respectively. That is, the polypeptide sequences FGALTAEKL and VALSCWLPL are most likely potential T cell epitopes for the APT-2 protein. The results also showed that 17-beta-HSD 10 contains multiple specific peptides that bind to MHC class II molecules and 81 specific P1 site anchoring bases. As the results showed, the strongest recognition sites in 17-beta-HSD 10 which related with HLA-DRB1_0701 and HLA-DRB5_0101 are amino acids 244 and 175 respectively. Besides, the polypeptide sequences FLNGEVIRL and VGMTLPIAR are most likely potential T cell epitopes for the 17-beta-HSD 10 protein.

The 3D-dimensional structures of the APT-2 protein and 17-beta-HSD 10 protein were analyzed by

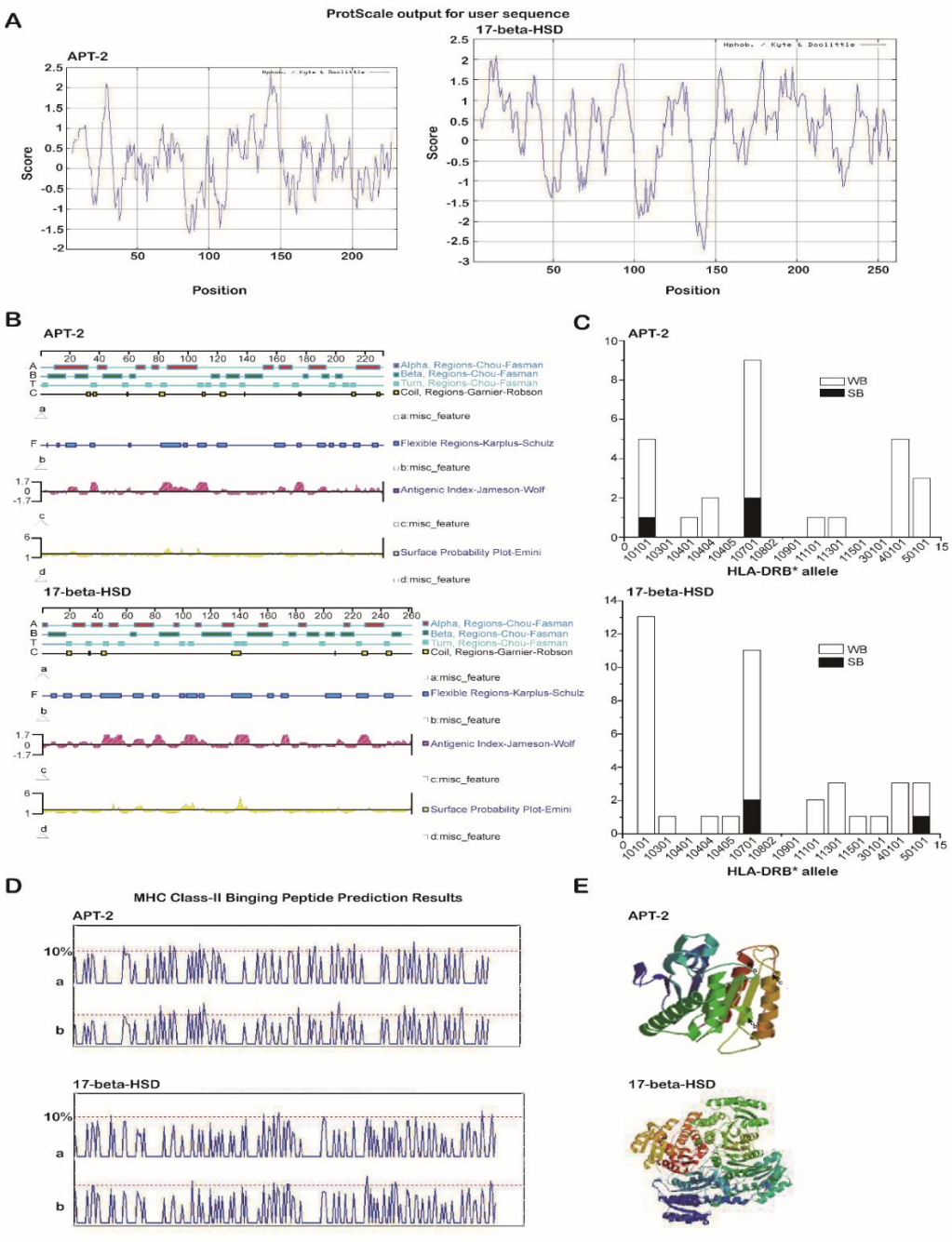

Fig4. *(A) Hydrophilic/hydrophobic analysis of APT-2 and 17-beta-HSD 10. (B) Analysis structures of ATP-2 and 17-beta-HSD 10 by Protean. a: the secondary structure of protein was predicted by Chou-Fasman and Gamier-*

Robson; b: the protein flexibility was predicted by Karplus-Schulz; c: the protein antigenic index was predicted by Jameson-Wolf; d: the protein surface accessibility was predicted by Emini. (C) The prediction of binding ability to MHC class II molecules of APT-2 and 17-beta-HSD 10. Correlation analysis between WB and SB and genotypes. Among them, WB has weak binding ability to MHC class II molecules (50< affinity(nM) <500) of the nonapeptide, SB is a nonapeptide with strong binding ability (affinity (nM) <50) to MHC class II molecules. (D) The MHC-II molecular specific ligand prediction in APT-2 and 17-beta-HSD 10 (In the picture above, a is for HLA-DRB1_0101, allele and b is for HLA-DRB1_0701, allele; while in the picture below, a is for HLA-DRB1_0701, allele and b is for HLA-DRB5_0101, allele). (E) The 3D-dimensional structures of APT-2 and 17-beta-HSD 10. The 3 active sites of APT-2 were shown with the black arrows in the picture above.

the online tool SWISS-MODEL (Fig. 4E). The results showed that 67% of the sequence of APT-2 has been determined (picture above). The 3 active sites of this protein are a (122), b (176), and c (210) residues, which play an important role in the charge relay system, as shown by the arrows in the picture. While 99% of the sequence of 17-beta-HSD 10 has been determined (picture below). The results also showed that the protein has 4 active sites: the nucleic acid binding region (position 1-42); the proton accepting region (position 168); the substrate binding site (position 155) and NAD binding site (position 172).

4. Discussion

We used two-dimensional gel electrophoresis (2-DE) to analyze differentially expressed proteins in QGY-7701 cells and QGY-7703 cells. After excluding significant impurities, 48 differential protein spots were found. The same method was used to analyze the differentially expressed proteins of QGY-7703 cells before and after cisplatin (CDDP) treatment, and 48 protein difference points were found. More importantly, we found two proteins that were deleted in QSG-7701 and CDDP-treated QGY-7703, while proteins specifically expressed in QGY-7703 cells were confirmed in the sample profiles prepared from three different lysates. Mass spectrometry identification showed that one of them was 17-beta-hydroxysteroid dehydrogenase 10 (17-beta-HSD 10), another basic property is Acyl-protein thioesterase 2 (APT-2). Bao et, al. used AACT combined with liquid chromatography-mass spectrometry for QSG-7701 hepatocytes and QGY-7703 to study the quantitative proteomics of liver cancer cells [26]. Based on the results of protein quantification, they analysed 141 proteins with altered expression, of which 73 were up-regulated in QGY-7703 expression and 68 were down-regulated but their results did not mention changes in APT-2 and 17-beta-HSD 10 expressed in QGY-7701 and QGY-7703 cells. In addition, the search MAPs are set in HEPG2_HUMAN and LIVER_HUMAN, and the differential protein information recorded by the isoelectric point and molecular weight were used to search in SWISS-2DPAGE database, there was no description of APT-2 or17-beta-HSD 10. So that the phenomenon of deletion of proteins is a new discovery.

In this study, the morphological characteristics and growth performance of QSG-7701and AGY-7703 were compared by HE staining and cell growth curves (Fig. 1B). It is believed that QSG-7701 hepatocytes already have certain characteristics of liver cancer cells and are in a critical period of transition from hepatocytes to cancer cells. HCC is r one of the malignant tumours with extremely high mortality, and the incidence rate is rising [27]. The use of proteomics to compare the protein expression profiles of normal cell lines and hepatocellular carcinoma cell lines with different biological behaviours is conducive to the discovery of changes in protein expression levels during the course of liver cancer progression, thereby facilitating early monitoring of tumours and guiding clinical treatment. We selected two cell lines, QGY-7703 liver cancer cells and QSG-7701 liver cells. Because they are from the same parent and have the same genetic background, they are good materials for studying the

mechanism of liver cancer using comparative proteomics. Shen et, al. compared the apoptosis rate, cell cycle and apoptotic index (Al) of three cell lines, such as QSG-7701 hepatocyte cell line, normal liver cell line (HL-7702) and hepatoma cell line (QGY-7703). QSG-7701 Hepatocyte cells have certain characteristics of liver cancer cells, but they are different from liver cancer cells and may belong to pre-cancerous cells that are being transformed [28].

The morphological changes of apoptosis are characterized by rounding, shrinking, and loss of microvilli, and adjacent cells are isolated; nuclear chromatin shrinks and accumulates to crescent-shaped, agglomerated or fragmented changes around the nuclear membrane; cytoplasm concentrates, endoplasmic reticulum expands into vesicular and cytoplasmic membrane fusion, mitochondria and lysosomes Keep intact; membrane invagination divides cells into multiple apoptotic bodies [29]. In the experiment, we first observed the number of cells in QGY-7703 cells treated with 2 μg/ml, 4 μg/ml, and 8 μg/ml CDDP by inverted microscope and HE staining. The cells showed a decrease in the number of cells, rounding of the cells, nuclear shrinkage and chromatin condensation, and were basically consistent with Shen et al. [28]. We observed the QGY-7703 cells before and after CDDP treatment by Hoechst 33324 fluorescence staining. Hoechst 33324 is a membrane-permeable fluorescent dye that can be inserted into the nucleus through the intact cell membrane and emit bright blue fluorescence when combined with the DNA of the nucleus. Normal cells and early-stage apoptotic cells can be stained by Hoechst 33324, but it is round and light blue of normal cell nucleus, while the nucleus of apoptotic cells is bright blue due to the concentration, and the nucleus is lobulated and crescent-shaped. We observed that 2μg/ml and 4 μg/ml CDDP-treated cells showed apoptosis in the nuclear margin and crescent (Fig. 2C), confirming the apoptosis of QGY-7703 cells after CDDP treatment.

In this paper, the inhibitory effect of CDDP on the proliferation of hepatocellular carcinoma cell line QGY-7703 and its related molecular mechanisms were studied. Proteomics was used to analyse the proteomics of QGY-7703 hepatoma cells after CDDP treatment. The results showed that CDDP can inhibit the proliferation of QGY-7703 and induce apoptosis of QGY-7703 and two specific expression proteins related to it by mass spectrometry were identified.

5. Conclusion

The morphology of hepatocyte cell QSG-7701 and hepatoma cell QGY-7703 were significantly different, but the growth characteristics were not significantly different, indicating that the proliferation of QSG-7701 hepatocyte cell line had some characteristics of tumour cell lines. The antitumour drug CDDP had a significant proliferation inhibitory effect on QGY-7703 cells, and induced tumour apoptosis.

48 differentially expressed proteins were found in QSG-7701 and QGY-7703 with or without CDDP treatment. The Acyl-protein thioesterase 2 and 17-beta-hydroxysteroid dehydrogenase 10 were identified to be missing expression in QSG-7701 and CDDP treated QGY-7703 but were expressed in QGY-7703. The results showed that these two proteins play an important role in the tumor development, indicating the possibility of applying in early detection and screening anti-hepatocarcinoma drugs as the targets.

Author Contributions

M.F and J.C designed the experiments for this study; J.C, P.Y and Y.F carried out the experiments and were involved in data acquisition and analysis. P.Y, J.C, G.C, B.D and M.F wrote and edited the manuscript. All the authors reviewed and acknowledged the manuscript.

REFERENCES

[1] Tang Z Y, Ye S L, Liu Y K, et al. A decade's studies on metastasis of hepatocellular carcinoma. J Cancer Res Clin Oncol, 2004, 130: 187-196

[2] Lee, J. Novel combinational treatment of cisplatin with cyclophilin A inhibitors in human hepatocellular carcinomas. Arch Pharm Res, 2010, 33: 1401-1409

[3] Tang Z Y, Yu Y Q, Zhou X D, et al. Subclinical hepatocellular carcinoma: an analysis of 391 patients. J Surg Oncol Suppl, 1993, 3: 55-58

[4] Lee C L, Hsiao H H, Lin C W, et al. Strategic shotgun proteomics approach for efficient construction of an expression map of targeted protein families in hepatoma cell lines. Proteomics, 2003, 3:2472-2486

[5] Srisomsap C, Sawangareetrakul P, Subhasitanont P, et al. Proteomic analysis of cholangiocarcinoma cell line. Proteomics, 2004, 4: 1135-1144

[6] Arancia G, Molinari A, Calcabrini A, et al. Intracellular P-glycoprotein in multidrug resistant tumor cells. Ital J Anat Embryol, 2001, 106: 59-68

[7] Chen F S, Cui Y Z, el al. Inhibition of sorafenib combined with cisplatin on hepatocellular carcinoma HepG2 cells. J South Med Univ, 2008, 28: 1684-1687

[8] Cui Y Z, Chen F S, Luo R C, el al. Effect of sorafenib on cisplatin-induced apoptosis of hepatocellular carcinoma HepG2 cells. Journal of Tropical Medicine, 2008, 8: 306-308

[9] Mohammad G. Cisplatin May Induce Frataxin Expression, 2003, 70: 367-371

[10] Schweyer S, Soruri A, Heintze A, et al.The role of reactive oxygen species in cisplatin-induced apoptosis in human malignant testicular germ cell lines. Int J Oncol, 2004, 25: 1671-1676

[11] Egan S E, Weinberg R A. The pathway to signal achievement. Nature, 1993, 365: 781-783

[12] Hoshino R, Tanimura S, Watanabe K, et al. Blockade of the extracellular signal-regulated kinase pathway induces marked G1 cell cycle arrest and apoptosis in tumor cells in which the pathway is constitutively activated: up-regulation of p27(Kip1). J Biol Chem, 2001, 276: 2686-2692

[13] Wasinger V C, Cordwell S J, Cerpa-Poljak, A, et al. Progress with gene-product mapping of the Mollicutes: Mycoplasma genitalium. Electrophoresis, 1995, 16: 1090-1094

[14] Seow T K, Ong S E, Liang R C, et al. Two-dimensional electrophoresis map of the human hepatocellular carcinoma cell line, HCC-M, and identification of the separated proteins by mass spectrometry. Electrophoresis, 2000, 21: 1787-1813

[15] Ou K, Seow T K, Liang R C, et al. Proteome analysis of a human heptocellular carcinoma cell line,HCC-M: an update. Electrophoresis, 2001, 22: 2804-2811

[16] Wang J, Zhu D, Ye X, et al. Establishment and some characteristics of a hepatoma cell line (QGY-7703). Chin. J. Oncol, 1981, 3: 241–244

[17] Zhu D, Wang J. The culture of the liver cell line QSG-7701, from a hepatoma donor, and its comparisonwith other hepatoma cell lines. Cancer Res. Prev. Treat, 1979, 6: 7–9

[18] Cheng S, Luo D, Xie Y. Taxol induced Bcl-2 protein phosphorylation in human hepatocellular carcinoma QGY-7703 cell line. Cell Biol Int, 2001, 25: 261-275

[19] L, Yi P, Wang Y, et al. Etoposide upregulates Bax-enhancing tumour necrosis factor-related apoptosis inducing ligand-mediated apoptosis in the human hepatocellular carcinoma cell line QGY-7703. Eur J Biochem, 2003, 270: 2721-2731

[20] Li J, Werner E, Hergenhahn M, et al. Expression profiling of human hepatoma cells reveals global repression of genes involved in cell proliferation, growth, and apoptosis upon infection with parvovirus H-1. J Virol, 2005, 79: 2274-2286

[21] R, Xing Z, Luan Z, et al. A specific splicing variant of SVH, a novel human armadillo repeat protein is up-regulated in hepatocellular carcinomas. Cancer Res, 2003, 63: 3775-3782

[22] Karkabounas S, Simos Y, et al. Anticancer and cytotoxic effects of a triorganotin compound with 2-mercapto-nicotinic acid in malignant cell lines and tumor bearing Wistar rats. Eur J Pharm Sci, 2011, 42: 253-261

[23] T, Chevallet M, Luche S, et al. Two-dimensional gel electrophoresis in proteomics: Past, present and future. J Proteomics, 2010, 73: 2064-2077

[24] Gorg A, Weiss W, Dunn M J. Current two-dimensional electrophoresis technology for proteomics.Proteomics, 2004, 4: 3665-3685

[25] Jenson O N, Wilm M, Shevchenko A. Methods in molecular biology.Totowa; Humana Press， 1999, 112:513-530

[26] Bao H, Song P, Liu Y, et al. Quantitative proteomic analysis of a paired human liver healthy versus carcinoma cell lines with the same genetic background to identify potential hepatocellular carcinoma markers. Proteomics Clin Appl, 2009, 3: 705-719

[27] P, Parkin D M, Bray F, et al. Estimates of the worldwide mortality from 25 cancers in 1990. Int J Cancer, 1999, 83: 18-29

[28] Shen L J, Guo W, Gao P, et al. The effects of p38MAPK and HBxAg on cell proliferation and apoptosis in human hepatocarcinogenesis. Zhonghua Gan Zang Bing Za Zhi, 2012, 20: 227-230

[29] Wyllie A H. Apoptosis: an overview. Br Med Bull, 1997, 53: 451-465

Citation: *Mao Fang, et.al. (2019). "The Morphology and Proteomics Variance Analysis of QSG-7701 and QGY-7703 Cell Lines after Cisplatin Treatment". International Journal of Clinical Chemistry and Laboratory Medicine (IJCCLM), 5(3), pp.6-18, DOI: http://dx.doi.org/10.20431/2455-7153.0503002.*